Co-extruded Polymeric Films for Gas Separation Membranes

Shannon R. Armstrong,[1] Grant T. Offord,[2] Donald R. Paul,[2] Benny D. Freeman,[2]
Anne Hiltner,[1] Eric Baer[1]

[1]Department of Macromolecular Science and Engineering, Center for Layered Polymeric Systems,
Case Western Reserve University, Cleveland, Ohio
[2]Department of Chemical Engineering, Center for Energy and Environmental Resources,
The University of Texas at Austin, Austin, Texas
Correspondence to: S.R. Armstrong (E-mail: sra10@case.edu)

ABSTRACT: In recent years, gas separation has become an important step in many production process streams and part of final products. Through the use of melt co-extrusion and subsequent orientation methods, gas separation membranes were produced entirely without the use of solvents, upon which current methods are highly dependent. Symmetric three layer membranes were produced using poly(ether-block-amide) (PEBA) copolymers, which serve as a selective material that exhibits a high CO_2 permeability relative to O_2. Thin layers of PEBA are supported by a polypropylene (PP) layer that is made porous through the use of two methods: (1) inorganic fillers or (2) crystal phase transformation. Two membrane systems, PEBA/(PP + $CaCO_3$) and PEBA/β-PP, maintained a high CO_2/O_2 selectivity while exhibiting reduced permeability. Incorporation of an annealing step either before or after orientation improves the membrane gas flux by 50 to 100%. The improvement in gas flux was a result of either elimination of strain induced crystallinity, which increases the selective layer permeability, or improvement of the PP crystal structure, which may increase pore size in the porous support layer. © 2013 Wiley Periodicals, Inc. J. Appl. Polym. Sci. **2014**, *131*, 39765.

INTRODUCTION

In recent years, gas separation membranes have become relevant due to their potential to improve process efficiency and reduce environmental impact. Membranes have found application in carbon capture, purification of synthesis byproducts and natural gas streams, flue gas separations, and modified atmosphere packaging.[1–5] Traditionally, the separation of gases has been achieved with methods dependent upon differences in molecular size, adsorption properties, or boiling points of the particular gases being separated.[6] The use of membranes in these processes has aided in lowering production costs by reducing the need for distillation equipment in gas separation and by enabling the capture and reuse of process byproducts.[7,8]

Materials for industrial membranes are chosen based on requirements of the process, which may include high permeability, high selectivity, chemical resistance, and mechanical and thermal stability. Many applications use porous ceramics or alloys due to good chemical resistance and high temperature stability; however, these membranes are difficult to produce, expensive, and cannot be easily adapted to various applications.[9,10] The shortcomings of ceramic and alloy membranes

make polymeric separation membranes attractive by comparison, making them a subject of intense study for the last several decades.

Advancements in the area of polymer-based separation membranes are largely due to material flexibility and developments in processing methods. Loeb and Sourirajan[11] were the first to produce an asymmetric membrane from cellulose acetate consisting of a dense layer supported by a porous layer. The methods used to fabricate these membranes and others are most often based on processes that use solvents in order to produce thin selective layers as well as the porous support layers that provide strength and stability to the membrane. Solution casting, interfacial polymerization, and solution coating have been used to produce selective layers with thicknesses less than 1 μm.[9,10] The porous support is often produced by phase inversion using polymers such as polysulfone, cellulose acetate, poly(vinylidene fluoride), or polyimide.[12] Some membranes are further supported with a non-woven polyester mat to provide additional stability.[9] These methods produce asymmetric membranes that have only one selective layer. If this layer develops small defects due to processing or as a result of handling,

convective transport through the defect may overwhelm solution-diffusion transport and thereby compromise the separation capability of the membrane. Although gas separation membranes have been produced by way of solvent based methods up to this point, there exists a need for methods that do not rely so heavily on solvents. Many of the solvents used are toxic, hazardous, and require strict protocols for safe disposal, thus resulting in a potentially unsafe and costly production process.

A novel advancement in separation membrane production has arisen with the ability to use forced assembly co-extrusion to produce films for use as gas separation membranes. Co-extrusion has numerous advantages over the traditional solvent-based membrane production methods. It is a continuous process, enabling rapid production of large quantities of membrane materials. The flexibility of the co-extrusion process enables the use of a variety of polymers and allows fine tuning of the layer structure and film properties. Our approach is to use co-extrusion of a highly selective polymer with a polymer, or polymer composite, that can easily be made porous. Post-processing orientation, another solventless process, is used to create porosity in the non-selective layer to serve as a high flux support for the thin selective polymer.
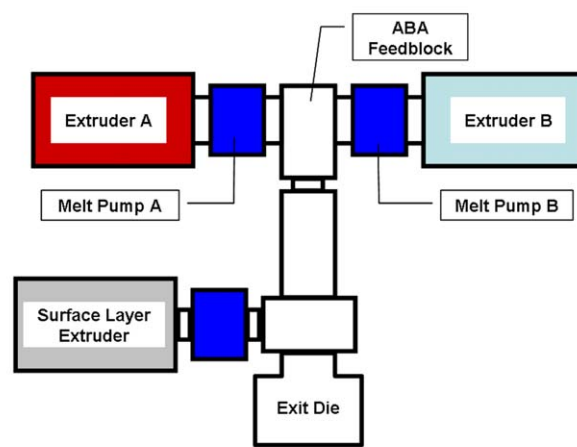
One possible application in which co-extruded membranes may prove beneficial is in the packaging of fresh produce, where tight control of package gas composition can extend shelf life and provide the capability of shipping around the world without spoilage. Generally, refrigeration is used as a method to preserve food; however, recently a new approach of controlling the atmosphere within the package, known as modified atmosphere packaging (MAP), has been developed. The package atmosphere is controlled by a membrane that has a CO_2/O_2 selectivity greater than unity. The gas composition inside the package, resulting from selective transport through the membrane, reduces the respiration rate of produce to levels that reduce the rate of degradation and yield a longer shelf life.[13,14] The best performance may be obtained by incorporating a material with a very high CO_2/O_2 selectivity into such a membrane. Specifically, polymers that exhibit strong interactions with quadrupolar CO_2 may prove advantageous in improving upon current MAP technology.[15]

MATERIALS AND METHODS

A poly(ether-block-amide) (PEBA) from the PEBAX xx33 series was purchased from Arkema in pellet form. Specifically, PEBAX 2533 (MFI = 12 g/10 min, 235°C/1.0 kg), which is a copolymer of 86 mol % polytetramethylene oxide (PTMO) and 14 mol % polyamide-12 (PA-12), was chosen for its relatively high CO_2/O_2 selectivity and high gas permeability.[16–19] Additionally, a polypropylene (PP) (H7012-35RN, MFI = 35 g/10 min, 230°C/2.16 kg) was purchased from Dow Chemical in pellet form and was chosen to have a matching viscosity with the PEBA to enable co-extrusion of quality films. Prior to co-extrusion, the PEBA was dried overnight under vacuum at 60°C to remove any water that may have been absorbed during storage.

Two different PP blends were produced using a Haake (Rheodrive 5000) twin screw extruder to ensure sufficient particle
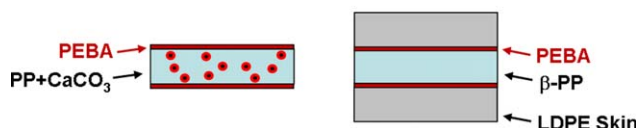

Figure 1. Schematic of the forced assembly multilayer co-extrusion process and layered films produced for use as gas separation membranes (PEBA/(PP + CaCO₃) and PEBA/β-PP). [Color figure can be viewed in the online issue, which is available at wileyonlinelibrary.com.]

dispersion in the PP matrix. The PP blends were made to enable the production of a porous film structure in post-extrusion orientation procedures. A blend of PP and inorganic filler was made containing 40 wt % filler, which included 96 wt % calcium carbonate ($CaCO_3$) and 4 wt % poly(ethylene oxide) (PEO; $M_n \sim 300$). $CaCO_3$ (Super-Pflex 200) with an average particle size of 0.7 μm and coated with 2 wt % stearic acid was provided by Specialty Minerals and the PEO was purchased from Sigma-Aldrich, both of which were used as received. Prior to melt blending, and co-extrusion, the $CaCO_3$ was dried overnight at 100°C under vacuum. A second blend was prepared by blending PP with 0.1 wt % of a known beta nucleating agent, quinacridone quinone (QQ; Sigma-Aldrich), to induce β-phase PP crystals. Each of the blends were subsequently used for co-extrusion against PEBA.

Two multilayer systems, PEBA/(PP + CaCO₃) and PEBA/β-PP, were produced at 190°C using a layer-multiplying co-extrusion process.[20,21] The co-extrusion system consisted of two extruders, an ABA feedblock, and a 14″ film die (Figure 1). For the films produced, PEBA layers were on the outside, creating a symmetric three layer structure. Volume compositions of 30/70 and 10/90, with PEBA as the low composition, were made by varying the relative melt pump rates of each material. PEBA/β-PP multilayer films were extruded with a low density polyethylene sacrificial skin layer, applied before the exit die, to reduce the cooling rate of the PP + QQ layers to ensure that the majority of the crystallinity was in the β-PP form rather than α-PP, which forms preferentially at lower temperatures. The skin layers accounted for 67% of the total film thickness. Additionally, a water-heated

film take off roll was operated at 95°C to further reduce the film cooling rate. The core film thickness, excluding the skin layers, was 50–100 μm for both systems, giving nominal PEBA layer thicknesses of 2.5–15 μm.

After co-extrusion of both material systems, PEBA/(PP + CaCO$_3$) and PEBA/β-PP, films were axially oriented to induce pore formation in the PP layer and reduce the PEBA layer thickness. Uniaxial orientation of PEBA/(PP + CaCO$_3$) films with a gauge length of 2.5 cm was conducted with an MTS Alliance RT/30 testing machine. Sample dimensions of 7 cm $\times$ 4 cm were used, with the smaller dimension parallel to the extrusion direction. Films were oriented along the extrusion direction at room temperature (21°C) with a strain rate of 50%/min to a maximum global strain of 250%. A Brückner Karo IV biaxial stretcher was used to biaxial orient PEBA/β-PP films with initial dimensions of 8.5 cm $\times$ 8.5 cm. Simultaneous stretching in the machine and transverse directions was conducted at 100°C with a strain rate of 100%/s to a draw ratio of 2 $\times$ 2. The sacrificial polyethylene skin layers were removed prior to orientation.

A cup test method was used to determine the relative water vapor transmission through the oriented PP composite films.[22] The measurement was set up by adhering the porous samples to a self-adhesive aluminum mask with a 5 cm^2 hole in the center. The aluminum mask was then attached to a petri dish using a two part epoxy. Once the epoxy had cured, 25 mL of water were added to the dish. The weight of the entire setup was monitored every hour for several days to determine the water loss over time and to compare the transmission rates of various porous films.

Permeability measurements were conducted on films and membranes with different thermo-mechanical histories: (1) as extruded, (2) oriented, and (3) annealed. Prior to all measurements, a self-adhesive aluminum mask was applied to both sides of the film. The aluminum mask possessed a 5 cm^2 hole in the center to allow for permeation testing and to provide a small enough sample area to prevent instrument sensor saturation. The O$_2$ and CO$_2$ permeabilities were measured using MOCON OX-TRAN 2/20 and PERMATRAN-C 4/40 permeation instruments. Testing was performed at 23°C and 0% humidity with a sample test area of 5 cm^2 for all samples. The O$_2$ and CO$_2$ test gases were used at 2% concentration in nitrogen to prevent sensor saturation due to high values of membrane flux.

Porous film surfaces and cross sections of layered film and membrane structures were observed through the use of scanning electron microscopy (SEM) (JEOL JSM-6510LV). Samples were embedded in a two part epoxy and cured overnight to aid in handling during imaging. To prevent smearing of the layers during cutting, a cryo-microtome (Leica EM UC7) was used at −110°C to cut all samples with a glass knife. After microtoming, a thin layer of gold ($\sim$10 nm) was sputter coated onto the microtomed surfaces.

RESULTS AND DISCUSSION

Membrane Materials Selection

Separation membranes made from porous metals, ceramics, or polymers separate gases based on size. Transport mechanisms such as Knudsen diffusion, Poiseuille flow, or surface diffusion dictate the permeability of such membranes. These membranes require very precise control of the pore size distribution in order to be efficient separators, particularly for micro- and ultra-filtration.[11] In dense polymeric films, separation occurs by differences between the solubility of gases and the rate at which those gases diffuse across the membrane, a mechanism known as solution-diffusion.[23] Composite membranes, which consist of a very thin dense polymeric layer supported by a thicker porous film, separate gases using this mechanism. These membranes are therefore able to perform separations requiring much higher selectivities than separations based on size alone.[10]

For the dense layer in a composite membrane to be effective in gas separation applications, it must possess two material properties: high selectivity and high permeability. Membranes with a high selectivity are more efficient separators and require fewer stages to achieve a given separation. In the case of MAP applications, high selectivity is required to reach desirable package compositions for some types of produce.[1] A sufficiently high permeability results in a smaller required membrane area and a greater allowable membrane thickness to achieve the required flux for the application. Choosing the correct material for the dense layer facilitates the design of the composite membrane, which typically performs best when it has the two following characteristics: (1) a sufficiently thin selective layer and (2) a highly porous support layer.[9,11] To create a membrane that meets these criteria, materials for the dense layer and the porous layer should be carefully chosen and studied independently prior to producing a composite film in order to determine the optimum conditions in which the necessary parameters can be achieved.

In membrane applications, it is most efficient to have a high selectivity in combination with a high gas flux, even within just the selective layer, which is generally the rate limiting step in membrane permeation. Unfortunately, there is a trade-off between these two requirements, thus creating an upper bound as described by Robeson.[21,24] Materials containing polar ether oxygen linkages, such as poly(ethylene oxide), are known to have a high CO$_2$ solubility due to strong interactions between ether oxygens and quadrupolar CO$_2$, resulting in high CO$_2$ to light gas selectivities and therefore demonstrating promise as solubility selective gas separation membranes.[25] Although PEO has a high selectivity ($\sim$15), a high amount of relatively impermeable crystalline phase (60 wt %) causes a low permeability that can be further reduced by formation of in-plane single crystals when confined in layers at the nano-scale.[26–29] From this example and the study done by Robeson, it is evident that high permeability will come at a cost to the selectivity. Although polyethers have been observed to possess high CO$_2$/O$_2$ selectivities, factors such as low permeability, low melting point, and high water sensitivity may restrict their use in some applications. Another approach must be taken to achieve a high selectivity and high flux.

To reduce the effects of crystallinity and water sensitivity, polyether containing copolymers, specifically poly(ether-block-amide)s, were investigated. PEBA is known to have a relatively high permeability along with a high selectivity of CO$_2$ to light
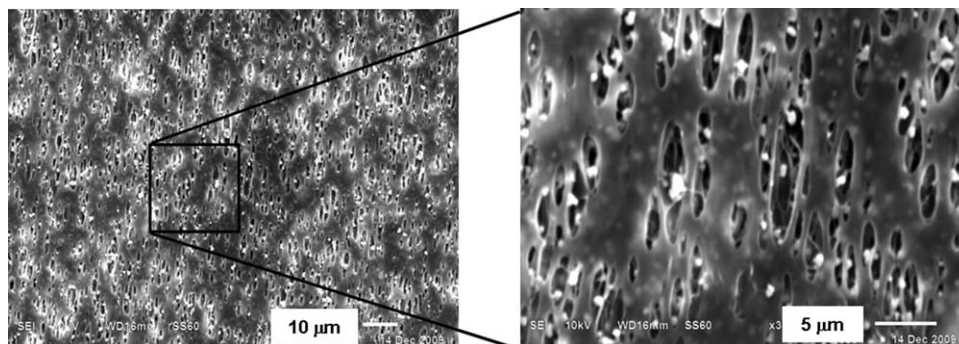
Figure 2. Porous PP + CaCO₃ created through uniaxial orientation at 23°C. Elongated pores with sizes of 0.5–3 μm $\times$ 3–7 μm are produced from cavitation around the CaCO₃ particles.

nonpolar gases, making it desirable in many gas separation applications.[16,18,19] The use of copolymers significantly reduces the crystallinity, thus improving gas flux while maintaining a selectivity comparable to the PEO homopolymer, particularly in copolymers of high polyether content. The use of poly(tetramethylene oxide) (PTMO), rather than PEO as the polyether block, allows additional improvement in permeability and reduction in water sensitivity.[30] The PTMO is amorphous due to a melting point below room temperature at 15°C, and has fewer ether groups making it less hydrophilic. From previous work, PEBA containing 86% PTMO demonstrated a CO_2/O_2 selectivity of 9.9 and relatively high oxygen permeability of 17.0 Barrer.[15] These values are higher than most traditional polymers, for which typical values are about 4 for selectivity and less than about 10 Barrer for permeability with a few materials being exceptions.[11,25] PEBA copolymers provide a good selectivity and permeability with the polyether soft blocks, while the polyamide blocks provide mechanical strength, both of which are necessary in membrane applications and will be beneficial in the current study.[31]

In addition to the separation layer, a support layer that provides strength and very little resistance to mass transfer is needed to structurally stabilize the thin, highly permeable and selective PEBA material. Several polymers have been shown to become porous when using specific processing methods, many of which are solvent based, such as phase inversion or dissolution of a component in polymer blends. In order to eliminate the dependence on solvents to produce a porous support structure, a mechanically based method is necessary. Several examples have been presented in the literature that make use of uniaxial or biaxial deformation of a polymer to induce porosity by way of crazing, delamination and cavitation, or phase transformation. Celgard is a commercially available porous PP that is created through a multistep process involving the crazing of α phase isotactic PP.[32] Due to the complexity of this process, it is not considered in this study, and two other techniques will be investigated.

A common method of forming porosity is to incorporate organic or inorganic fillers which delaminate from the polymer matrix, such as polypropylene (PP) and polyethylene (PE), upon deformation.[33,34] In this study, calcium carbonate (CaCO₃) was melt blended into PP, extruded, and uniaxially oriented resulting in cavitation through delamination of the CaCO₃ particles from the PP matrix and is apparent by observation of the elongated pores surrounding the particles (Figure 2). With sufficiently high filler content, the cavitated regions become interconnected and produce a porous matrix with low resistance to gas flow.[35]

Studies have been performed on the variables that affect the porosity and film strength of CaCO₃ filled PP, such as filler content, particle size, filler/matrix adhesion, orientation temperature, and strain rate.[36] Galeski et al.[37,38] determined that an optimum particle size of approximately 1 μm coated with stearic acid and at a filler content of 40 wt % produced highly porous and mechanically robust films. Incorporation of a low molecular weight PEO ($M_n = 300$) into the PP + CaCO₃ blend prevented premature film fracture during orientation, particularly at high filler content, by coating the CaCO₃ particles and aiding in dispersion, thus preventing aggregation of the CaCO₃ into large particles. Upon orientation, the films become white in color due to the random scattering of light from the newly formed pores, which is a good visual indicator of porosity. Through use of the cup test method, previously used by Mueller, a relative water vapor transmission rate was measured to qualitatively compare the porosity levels of various PP + CaCO₃ substrates.[21] From the cup test data, a filler content of 40 wt % containing 4 wt % PEO surfactant and uniaxially oriented at 23°C and 50%/min to a strain of 250%, produced the most porosity with pore sizes from 3 to 7 μm while maintaining film strength, both during and after deformation.

An alternate method for producing porous PP is with the use of nucleating agents that produce β phase isotactic PP. β-PP has been found to become porous when uniaxially or biaxially oriented over a range of conditions.[39,41] In the current study, quinacridone quinone (QQ) was used as the β nucleator and is known to be highly efficient at nucleating β phase PP at relatively low concentrations (<0.1 wt %).[40] Many factors influence the porosity of β-PP, including the β crystallinity and orientation conditions. Sufficient β crystallinity is needed to produce porosity, which results from void formation between lamellae caused by the applied stress, and is accompanied by a transformation of the β phase to the α phase.[41] To ensure the formation of β-PP in the extruded films, the cooling rate was carefully controlled during extrusion and film take-off.
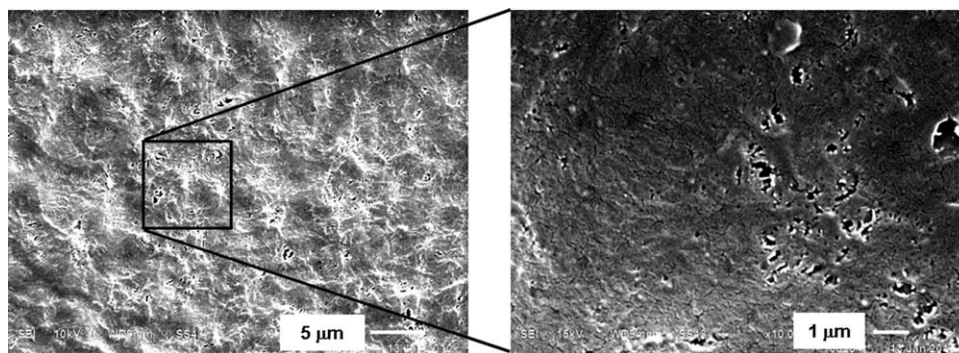
Figure 3. Porous β-PP created through biaxial orientation at 100°C to a draw ratio of 2 × 2. Pore sizes of less than 300 nm were produced.

Although uniaxial and biaxial orientation have been shown to produce porosity in β-PP, the current work focuses on biaxial orientation because it is believed that films with larger pores and a more uniform porous structure would be achieved.[42] The biaxial orientation conditions (temperature, strain rate, and draw ratio) were varied to produce porous β-PP films, which were further tested using the cup test to determine the optimum stretching conditions. Visual inspection of the degree of change between the translucent dense films and the white/opaque porous membranes gives an indication of the amount of possible porosity, later confirmed with the cup test and permeation measurements. Orientation temperatures of 90°C produced higher fluxes; however, the film uniformity was not as good and, thus, this condition was not used for the final membrane.[43] Films that were biaxially oriented at 100°C with a strain rate of 100%/s and 2 × 2 draw ratio were found to have the highest porosities, with pore sizes visible at the surface on the order of 20 to 300 nm (Figure 3).

Figure 4. Normalized water vapor transmission through porous PP + CaCO₃ and β-PP films compared to Celgard 2500, a commercially produced porous PP. [Color figure can be viewed in the online issue, which is available at wileyonlinelibrary.com.]

Using the cup test, PP + CaCO₃ and β-PP porous films, which were created at the optimum orientation conditions, were compared to Celgard 2500, a commercially produced porous PP (Figure 4). Based on the normalized water loss for each porous film sample, the PP + CaCO₃ porous membrane showed comparable water vapor transmission to the Celgard membrane. On the other hand, the β nucleated PP exhibited a transmission that was about half that of the Celgard. This may be a result of the difference in pore size between each of the films, in which the β-PP pores are <100 nm while the Celgard pores are 50–200 nm and the PP + CaCO₃ pores are on the micron scale.[43,44] Differing pore formation mechanisms may also explain the disparity in porosity. Although the β-PP film appears much lower in porosity, it is believed that there is still promise in its use as a membrane support layer due to previous work demonstrating the effects of processing conditions on the porosity.[43] Knowing that PP + CaCO₃ and β-PP can be made significantly porous and that PEBA copolymers possess good CO_2/O_2 selectivity and high flux, there is an opportunity to combine these components to create separation membranes, specifically for modified atmosphere packaging, using a solventless co-extrusion and orientation process.
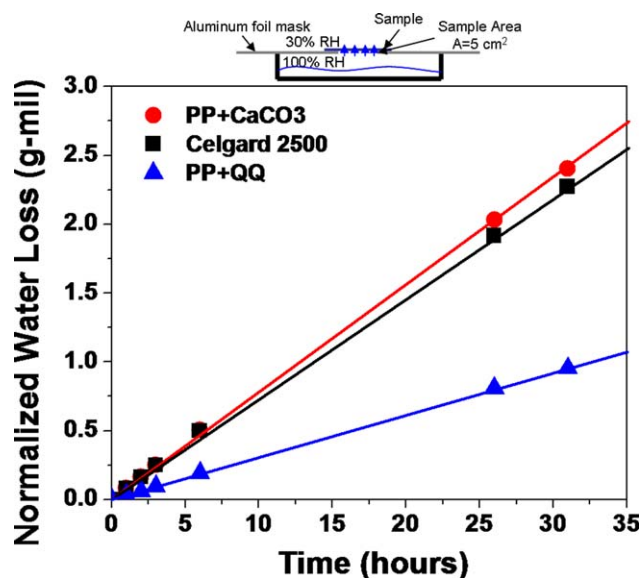
As-extruded Three Layer Films
Forced assembly co-extrusion, an entirely solventless process, was used to produce symmetric three layer films with the outer layers being the selective PEBA material. A symmetric structure is used for two reasons. First, the existence of two selective layers allows retention of the selectivity even if one layer has a defect. Second, the difference in elasticity between PP and PEBA will cause curling and buckling of an asymmetric membrane structure. The core layer consists of a PP composite, either PP + CaCO₃ or β-PP that is capable of becoming porous upon orientation. These films are to be subsequently used for separation membranes after incorporating an orientation processing step after co-extrusion. To produce quality gas separation membranes, the initial co-extruded films must have uniform layer and film thicknesses. This was accomplished by having matching viscosities between the PEBA and the PP composites. For each co-extruded system, the films had uniform layers with both of the PEBA layers being of similar thicknesses, which were supported by a thick PP layer in the center, as observed by SEM (Figure 5). At this point, the PP layers are solid films and
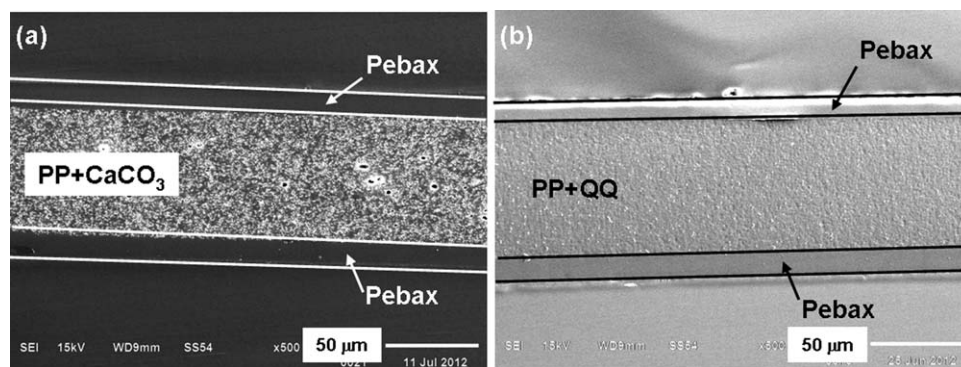
Figure 5. As-extruded symmetric three layer films of 30/70 volume composition. (a) PEBA/(PP + CaCO$_3$) and (b) PEBA/β-PP

display no porosity. As a result, the composite film has a measured CO$_2$/O$_2$ selectivity of 4 because the PP layer, with a measured oxygen permeability of 0.9 Barrer, is controlling the rate of mass transfer through the film. To achieve a high flux and increase the selectivity to near that of the PEBA material, either uniaxial or biaxial orientation is applied to the PEBA/(PP + CaCO$_3$) or PEBA/β-PP films to reduce the mass transfer resistance imposed by the PP layer.

Gas Separation Membranes from Co-extruded Films

Films produced by solventless co-extrusion are nonporous. Extruded polymer films have relatively low gas flux because flux, J, varies inversely with thickness, t,:

$$J = \frac{P \Delta p}{t} \tag{1}$$

Minimizing the thickness of the membrane, therefore, results in greater gas throughput, but reducing the thickness of the separating layer presents a fabrication challenge. In addition to the difficulty of making such films, as film thickness is reduced, the mechanical strength of the film is significantly diminished. It is for this reason that traditional dense film membranes relying on the solution-diffusion mechanism are produced with the necessarily thin selective layer atop a sufficiently thick porous material. Work done by Liu et al.[45] demonstrated a solvent-based process of producing ultra-thin PEBA membranes (0.7 μm) that required a PSF substrate for stability during permeation testing. There have been additional studies using various PEBA copolymers for membrane applications, many of which used solvent casting.[46–48] Combining the selective and support layers during

extrusion is one potential avenue to bypass the challenges of producing ultrathin films.

As previously described, two solventless methods for making porous PP can be used. In order to successfully produce high flux, high selectivity membranes from co-extruded films, it is necessary that the PEBA selective layers are not damaged by the PP composite layers during orientation. SEM was used to qualitatively observe the cross-sections of multilayer films after orientation. PEBA/(PP + CaCO$_3$) films clearly show that the PP layer has become porous in films of 10/90 and 30/70 volume compositions (Figure 6). The pore structure appears similar to the porous PP + CaCO$_3$ film that was produced without the PEBA layers, with an open cavity surrounding the CaCO$_3$ particle. Additionally, the PEBA layers in the 30/70 composition tend to delaminate from the PP + CaCO$_3$ during microtoming. This is due to relatively poor adhesion between the PEBA and PP, which is further reduced upon pore formation due to lower contact surface area.

Porosity is not as obvious in images of PEBA/β-PP films after biaxial orientation as in the case of the PP + CaCO$_3$ system. The pore size produced by biaxial orientation of β-PP is significantly smaller than that produced by uniaxial orientation of PP + CaCO$_3$, thus making observation of the pore structure more difficult (Figure 7). Magnified images show a somewhat layered structure with elongated pores. A benefit of the orientation process is a reduction of PEBA layer thickness, as seen in the SEM images, which will provide an increase in membrane flux.
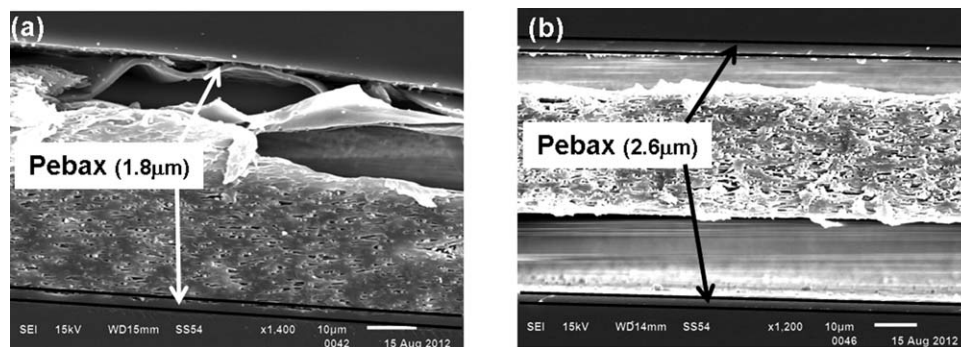

Figure 6. Uniaxially oriented PEBA/(PP + CaCO$_3$) films. (a) 10/90, (b) 30/70 volume composition.
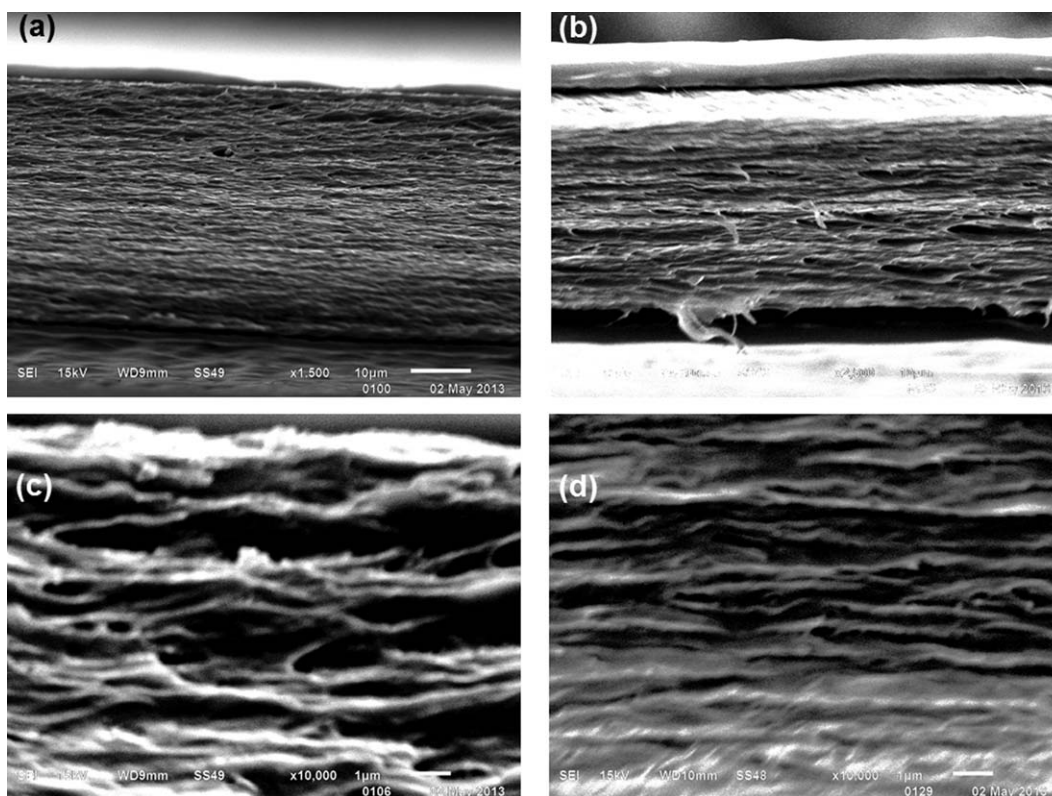
Figure 7. Biaxially oriented PEBA/β-PP films at low and high magnification. (a,c) 10/90 and (b,d) 30/70 volume composition.

To quantitatively determine how successful the uniaxial or biaxial orientation was in producing a porous substrate and maintaining PEBA layer integrity, the O_2 and CO_2 gas flux through each membrane was measured. It is useful to express the gas transport rates through these films as a permeance rather than as a permeability in order to compare the membrane composites on a total flux basis. Permeance is expressed in this study in gas permeation units (GPU), which are equivalent to 1 Barrer/μm. The highest values of permeance result from membranes made from materials with high permeability and made as thin as possible, which are more desirable from an application point of view. Examination of the flux data for PEBA/(PP + CaCO$_3$) and PEBA/β-PP membranes show that permeances increased in a similar fashion as the total PEBA thickness was reduced, as would be expected based on the previous discussion and eq. (1) (Figure 8). By assuming that the PP support layer imposes no resistance to mass transfer and that the selective PEBA layer performs identically to that of an extruded control film, multilayered membrane transport performance can be compared to the performance of PEBA control film. Based on these ideal assumptions, measured values are less than expected; however, a CO_2/O_2 selectivity of at least 7 was maintained for all membranes, as compared to 4 for some commercial membranes.

Pebax/(PP + CaCO$_3$) Membranes

Since the expected membrane flux values were not achieved with either pore formation technique, there is likely to be a correlation between the production conditions, the structures pro-

duced, and the resultant properties. The observed transport properties can be a result of unexpected structural changes attributed to either the PP or PEBA layers upon film orientation. If low levels of porosity are created in the PP layer, reduced permeability will result due to a non-negligible resistance to mass transfer through the membrane. To determine whether low PP porosity is the culprit for low flux, the PEBA layers were carefully removed from the PP + CaCO$_3$ after uniaxial orientation and the cup test was used to measure water vapor transmission through the PP. Comparison of the vapor transmission rate of porous PP from a multilayer membrane to the porous PP + CaCO$_3$ produced without PEBA layers shows that PP + CaCO$_3$ from the layered membrane was about half that of the control porous PP + CaCO$_3$ film (Figure 9). It is possible that the presence of the PEBA layers prevent some pore formation at the PP surface, or that elastic recovery of the PEBA layers may close some of the pores, thus increasing the resistance to gas flow.

Using the same delamination method, the PEBA layers were carefully removed from the PP + CaCO$_3$ support layer for measurement of the PEBA CO_2 and O_2 permeability. The PEBA layers were expected to exhibit O_2 permeability values that are the same as values measured for bulk control films [$P(O_2) = 17$ Barrer]. Upon measurement of the permeability, values of approximately 9 Barrer were found, a significant reduction relative to the control films. This finding provides evidence that a change in the PEBA layers is also a culprit for reduced membrane flux upon uniaxial orientation. A previous study observed
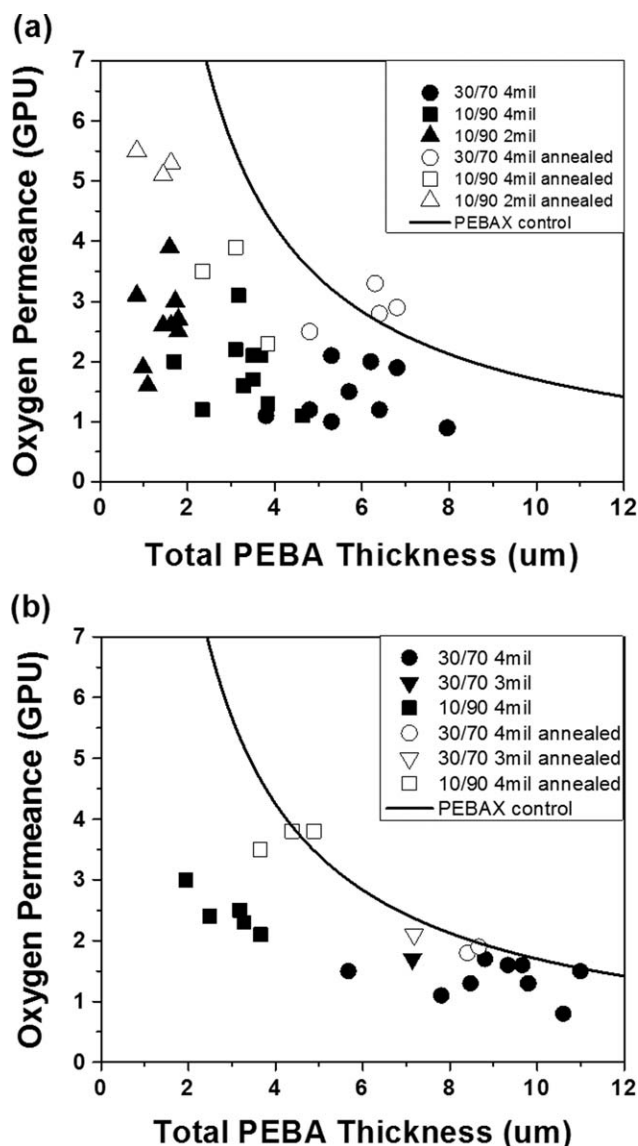
Figure 8. Oxygen permeance of (a) PEBA/(PP + CaCO₃) and (b) PEBA/β-PP three-layer membranes with and without annealing.

Figure 9. Normalized water vapor transmission through porous PP + CaCO₃ and β-PP films oriented with and without PEBA layers, as well as annealed β-PP from a three layer membrane. Celgard 2500 results are also presented for comparison. [Color figure can be viewed in the online issue, which is available at wileyonlinelibrary.com.]

The incorporation of an annealing step after uniaxial orientation of the PEBA/(PP + CaCO₃) membranes resulted in a large increase in the flux. Both the O_2 and CO_2 flux increased approximately 60–100% after annealing for both 30/70 and 10/90 membrane compositions (Table I). The increase in flux allowed the permeability to recover to near the PEBA control values and approaches the expected trend line for membranes that exhibit high flux through the support layer. Additionally, the selectivity showed some improvement with annealing (Table II). These results demonstrate that the post-processing orientation conditions are important and directly affect the final membrane properties through changes in the PEBA structure.

Knowing that strain induced crystallinity of the PEBA occurs during room temperature orientation, two approaches could be used in the membrane production process to avoid reductions in flux. First, an annealing step can be incorporated after orientation to remove PEBA crystallinity, as was used in the current study. Second, the orientation conditions can be altered, such as increasing the drawing temperature, so that strain induced crystallization of the PTMO blocks is prevented. Increasing the orientation temperature to 50–60°C prevents PTMO crystallization while maintaining the ability to produce high porosity in the PP+CaCO₃ support layer.

Pebax/β-PP Membranes

In the previously discussed PEBA/(PP + CaCO₃) system, the majority of the reduced flux was attributed to strain induced

similar trends in permeation for PEBA materials in which the permeability decreased linearly with increasing strain. This result was attributed to strain induced crystallinity of the polyether block of the PEBA copolymer, and therefore, the effect was most evident in copolymers with high levels of poly(tetramethylene oxide).[15] Through the use of differential scanning calorimetry (DSC), the melting temperature of residual strain induced PTMO crystallinity was determined to be 42°C, correlating well with the equilibrium melting temperature of highly aligned PTMO chains. Incorporation of an annealing process above this temperature allows the PTMO crystallinity to be removed through relaxation of the aligned polymer chains. After annealing, the permeability was found to increase to values comparable to the unoriented control films. Based on this study, a post-orientation annealing step was incorporated into the membrane production process.
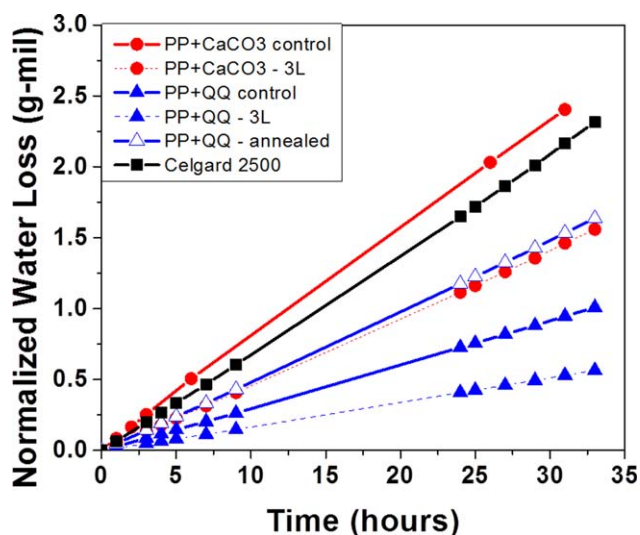
Table I. Oxygen Permeance (GPU) of PEBA/(PP + CaCO₃) Membranes

	30/70	10/90	
Initial Film Thickness (μm)	100	100	50
As-extruded	1.4	1.8	3.0
Annealed	2.9	3.2	5.3

Table II. CO_2/O_2 Selectivity of PEBA/(PP + CaCO$_3$) Membranes

	30/70	10/90	
Initial Film Thickness (μm)	100	100	50
As-extruded	8.7	8.7	8.0
Annealed	9.6	8.7	8.5

Table IV. CO_2/O_2 Selectivity of PEBA/β-PP Membranes

	30/70		10/90
Initial Film Thickness (μm)	100	75	100
As-extruded	7.3	6.3	7.4
Annealed (post-orientation)	8.7	–	–
Annealed (pre-orientation)	8.7	5.4	7.9

crystallization of the polyether blocks within the PEBA layers. To determine whether this phenomenon also plays a part in the observed flux values for the PEBA/β-PP system, membranes were annealed at 60°C, as was used previously. Interestingly, the membrane permeability did not change upon annealing, exhibiting flux values that were the same as prior to annealing (Table III). This result demonstrates that strain induced crystallization does not occur in this system, possibly for two reasons. First, film orientation was conducted at 100°C, which is well above the melting temperature of PTMO strain induced crystallinity ($T_m = 42°C$), which prevented the formation of PTMO crystals. Second, biaxial orientation, rather than uniaxial orientation, was used and may have inhibited the PTMO soft blocks from aligning in one direction and strain crystallizing. Biaxial orientation applies stress on the polymer in two directions, reducing the degree of packing and alignment that occurs during strain induced crystallization. The lack of an annealing effect on the flux of PEBA/β-PP membranes shifts the focus from the PEBA selective layers to the PP support layer.

Based on the previous observation, it was concluded that the deviation in gas flux is most likely due to low porosity in the PP layers and not orientation of the PEBA layers. To improve the overall membrane gas flux, it is necessary that the β-PP layer exhibit less resistance to gas flow, which can be achieved by increasing the porosity. Since pore formation in β-PP occurs as a result of lamellar separation and dissipation of stress by cavitation during deformation, the number of pores created will be directly related to the amount of β-PP crystallinity. Although the co-extrusion conditions were optimized to allow β-PP to crystallize, the cooling rate may still not be slow enough to allow the maximum amount and size of β-PP crystallinity to form. It is possible to further improve the β-PP crystallinity through annealing at a temperature that favors the formation of the β-PP crystal structure. Annealing temperatures of 120–140°C have been shown to improve the amount and the structure of β-PP crystallinity.[40,49]

Based on prior studies regarding the annealing of β-PP, PEBA/β-PP co-extruded films were annealed at 140°C for 30 min to allow the β-PP structure to be further improved. After anneal-

Table III. Oxygen Permeance (GPU) of PEBA/β-PP Membranes

	30/70		10/90
Initial Film Thickness (μm)	100	75	100
As-extruded	1.4	1.7	2.6
Annealed (post-orientation)	1.0	–	–
Annealed (pre-orientation)	1.9	2.1	3.7

ing, the films were biaxially oriented under the same conditions used previously. Upon measurement of the flux, the observed values were improved 30% over the non-annealed membranes with the selectivity also showing some improvement (Tables III and IV). This result aligns well with previous work demonstrating that annealing prior to orientation leads to a higher flux by producing a less tortuous path for gas flow.[41] The improvement in β-PP flux caused the membrane flux values to approach that of the expected values. Additionally, the flux through the β-PP support layer is now comparable to that of the PP + CaCO$_3$ porous support (Figure 9).

Although the incorporation of an annealing process significantly improves the gas flux through each membrane system, additional improvement is necessary for broad application of these membranes. Examination of the flux data shows that as the PEBA thickness decreases the flux deviates farther from the ideal values, possibly a result of decreasing porosity in the PP support layer or high orientation of the PEBA. Additionally, each system reaches a minimum in PEBA thickness at which production of the membranes was successful. The PEBA/(PP + CaCO$_3$) membranes can be fabricated as thin as approximately 1 μm in PEBA thickness, after which the PEBA layers do not remain intact after orientation. It is possible that at this thickness the PEBA layers are being punctured by the CaCO$_3$ particles (0.7 μm diameter). The PEBA/β-PP system can only be produced as thin as a few microns in PEBA thickness; however, a different issue is the culprit in these membranes. As the PEBA/β-PP film thickness is reduced, the cooling rate is increased during film extrusion and may prevent the necessary amount of β-PP crystallinity from forming. Films less than about 80 μm did not stretch uniformly and tended to fracture during biaxial orientation, possibly due to low β-PP crystallinity. Since the porosity is directly dependent on the amount of β-PP crystallinity, high levels of crystallinity are necessary to produce high porosity and, thus, high gas flux. Commercial extrusion lines should be able to avoid this issue through better control of temperature during film take off and would eliminate the need for the sacrificial LDPE skin layers.

CONCLUSIONS

Through the use of multilayer co-extrusion and axial orientation, highly selective and moderately high flux symmetric membranes were successfully produced entirely without the aid of solvents. Both systems, PEBA/(PP + CaCO$_3$) and PEBA/β-PP, maintained a CO_2/O_2 selectivity of at least 7, which is approximately double that of commercial materials being used for modified atmosphere packaging. The gas flux values tended to deviate from that expected of an ideal composite membrane

owing to two different factors. First, PEBA/(PP + CaCO$_3$) membranes demonstrated strain induced crystallinity of the PEBA layers due to uniaxial orientation at temperatures below the equilibrium melting of the PTMO soft blocks of the PEBA. Post-orientation annealing allowed the permeability to significantly improve through melting of the PTMO without subsequent recrystallization. Second, PEBA/β-PP showed low porosity in the β-PP that could be increased through annealing prior to orientation by improvement of the amount and size of β-PP crystals.

The processing conditions proved to be highly important to the final membrane fluxes as was demonstrated through the use of annealing to alter the structure of each membrane component and subsequently the observed membrane properties. This study demonstrates that a solventless process can be successfully used to produce separation membranes, thus, improving the processing conditions, cost, and environmental impact. Continued work is being conducted to further improve the flux of co-extruded membranes by optimizing the co-extrusion and orientation conditions to provide a viable alternative to solution processed membranes in a variety of applications, including modified atmosphere packaging.

ACKNOWLEDGMENTS

REFERENCES

1. Kirkland, B. S.; Clarke, R.; Paul, D. R. *J. Membr. Sci.* **2008**, *324*, 119.

2. Rodriguez-Aguilera, R.; Oliveira, J. C. *Food Eng. Rev.* **2009**, *1*, 66.

3. Al-Ati, T.; Hotchkiss, J. H. *J. Agric. Food Chem.* **2003**, *51*, 4133.

4. Merkel, T. C.; Lin, H.; Wei, X.; Baker, R. W. *J. Membr. Sci.* **2010**, *359*, 126.

5. Scholes, C. A.; Kentish, S. E.; Stevens, G. W. *Recent Pat. Chem. Eng.* **2008**, *1*, 52.

6. Toshima, N. Ed. *Polymers for Gas Separation.* VCH: New York, **1992**.

7. Baker, R. W.; Wijmans, J. G.; Kaschemekat, J. H. *J. Membr. Sci.* **1998**, *151*, 55.

8. Bernardo, P.; Drioli, E.; Golemme, G. *Ind. Eng. Chem. Res.* **2009**, *48*, 4638.

9. Scott, K.; Hughes, R. Eds. *Industrial Membrane Separation Technology.* Blackie Academic and Professional: London, **1996**.

10. Paul, D. R.; Yampol'skii, Y. P. Eds. *Polymeric Gas Separation Membranes.* CRC Press: Boca Raton, **1994**.

11. Loeb, S.; Sourirajan S. *Saline Water Conversion II. ACS Advances in Chemistry Series 38.* American Chemical Society: Washington, DC, **1963**; pp 117–132.

12. Baker, R. W. *Membrane Technology and Applications*, 2nd ed.; Wiley: New York, **2004**.

13. Paul, D. R.; Clarke, R. *J. Membr. Sci.* **2002**, *208*, 269.

14. Kirkland, B. S.; Clarke, R.; Paul, D. R. *J. Membr. Sci.* **2008**, *324*, 119.

15. Lin, H.; Freeman, B. D. *J. Mol. Struc.* **2005**, *739*, 57.

16. Armstrong, S.; Freeman, B. D.; Hilner, A.; Baer, E. *Polymer* **2012**, *53*, 1383.

17. Rezac, M. E.; John, T.; Pfromm, P. H. *J. Appl. Polym. Sci.* **1997**, *65*, 1983.

18. Bondar, V. I.; Freeman, B. D.; Pinnau, I. *J. Polym. Sci. Part B: Polym. Phys.* **1999**, *37*, 2463.

19. Bondar, V. I.; Freeman, B. D.; Pinnau, I. *J. Polym. Sci. Part B: Polym. Phys.* **2000**, *38*, 2051.

20. Bernal-Lara, T. E.; Ranade, A.; Hiltner, A.; Baer, E. In *Mechanical Properties of Polymers Based on Nanostructure*, 1st ed.;, Micheler, G. H., Balta-Callaja, F., Eds.; CRC Press: Boca Raton, FL, **2005**.

21. Ponting, M.; Hiltner, A.; Baer, E. *Macromol. Symp.* **2010**, *294-I*, 19.

22. Mueller, C.; Topolkaraev, V.; Soerens, D.; Hiltner, A.; Baer, E. *J. Appl. Polym. Sci.* **2000**, *78*, 816.

23. Wijmans, J. G.; Baker, R. W. *J. Membr. Sci.* **1995**, *107*, 1.

24. Robeson, L. M. *J Membr. Sci.* **2008**, *320*, 390.

25. Lin, H.; Van Wagner, E.; Raharjo, R.; Freeman, B. D.; Roman, I. *Adv. Mater.* **2006**, *18*, 39.

26. Pethe, V. V.; Wang, H. P.; Hiltner, A.; Baer, E.; Freeman, B. D. *J. Appl. Polym. Sci.* **2008**, *110*, 1411.

27. Brandup, J.; Immergut, E. H. Eds. *Polymer Handbook, 3rd ed.;* Wiley: New York, **1989**; Chapter 6.

28. Wang, H.; Keum, J. K.; Freeman, B. D.; Hiltner, A.; Baer, E.; Rozanski, A.; Galeski, A. *Science* **2009**, *6*, 575.

29. Lin, Y.; Hiltner, A.; Baer, E. *Polymer* **2010**, *51*, 4218.

30. Li, H.; Freeman, B. D.; Ekiner, O. M. *J. Membr. Sci.* **2011**, *369*, 49.

31. Kim, J. H.; Ha, S. Y.; Lee, M. Y. *J. Membr. Sci.* **2001**, *190*, 179.

32. Druin, M. L.; Loft, J. T.; Plovan, S. G. Novel Open-celled Microporous Film. US Pat. 3,801,404, **1974** (Celanese Corporation).

33. Hetzler, K. G.; Jacobs, R. L. Oriented Polymeric Microporous Films with Flexible Polyolefins. US Patent 5,910,136, **1999** (Kimberly-Clark Worldwide, Inc.).

34. Dubnikova, I. L.; Muravin, D. K.; Oshmyan, V. J. *Polym. Eng. Sci.* **1997**, *37*, 1301.

35. Hale, W. R.; Dohrer, K. K.; Tant, M. R.; Sand, I. D. *Colloids Surf* **2001**, *187–188*, 483.

36. Kundu, P. P.; Choe, S. *Polym. Rev.* **2003**, *43*, 143.

37. Galeski, A.; Kryszewski, M.; Kowalewski, T. *Polym. Eng. Sci.* **1992**, *32*, 1217.

38. Kryszewski, M.; Galeski, A.; Kowalewski, T. *Polymer Composites.* B Sedlacek, Walter de Gruyter & Co.: Berlin, New York, **1986**; pp 141–152.

39. Ran, S.; Xu, M. *Chinese J. Polym. Sci.* **2004**, *22*, 123.

40. Fujiyama, M. *Inter. Polym. Proc.* **1996**, *3*, 271.

41. Offord, G. T.; Armstrong, S. R.; Paul, D. R.; Freeman, B. D.; Hiltner, A.; Baer, E.; Swinnea, J. *Polymer* **2013**, *54*, 2577.

42. Chu, F. *Polymer* **1996**, *37*, 573.

43. Offord, G. T.; Armstrong, S. R.; Freeman, B. D.; Hiltner, A.; Baer, E.; Paul, D. R. *Polymer* **2013**, *54*, 2796.

44. Celgard Product Literature.

45. Liu, L.; Chakma, A.; Feng, X. *J. Membr. Sci.* **2004**, *235*, 43.

46. Louie, J. S.; Pinnau, I.; Ciobanu, I.; Ishida, K. P.; Ng, A.; Reinhard, M. *J. Membr. Sci.* **2006**, *280*, 762.

47. Marcq, J.; Nguyen, Q. T.; Langevin, D.; Brule, B. *Environ. Prot. Eng.* **2005**, *31*, 13.

48. Sijbesm, H.; Nymeijer, K.; van Marwijk, R.; Heijboer, R.; Potreck, J.; Wessling, M. *J. Membr. Sci.* **2008**, *3*, 263.

49. Bai, H.; Wang, Y.; Zhang, Z.; Han, L.; Li, Y.; Liu, L.; Zhou, Z.; Men, Y. *Macromolecules* **2009**, *42*, 6647.